Bone Marrow Tumor Microenvironment of Obese Hodgkin Lymphoma Patients: implications of insulin axis

Andreia Matos (✉ andreia.matos@i3s.up.pt)

 i3S - Health Research and Innovation Institute

Joana Marinho-Dias

 Portuguese Oncology Institute of Porto (IPO Porto)

Sofia Ramalheira

 Hospital Center of Vila Nova de Gaia/Espinho

Susana Roncon

 Portuguese Oncology Institute of Porto (IPO Porto)

Dulcineia Pereira

 Portuguese Oncology Institute of Porto (IPO Porto)

Carla Rodrigues

 Portuguese Oncology Institute of Porto (IPO Porto)

Mário Mariz

 Portuguese Oncology Institute of Porto (IPO Porto)

Ana Miranda

 Sta. Maria Hospital

Helena Brízido

 Germano de Sousa Laboratory Medicine Center

Manuel Bicho

 Faculdade de Medicina, Universidade de Lisboa

Pingzhao Hu

 Western University

Flávia Pereira

 i3S - Health Research and Innovation Institute

Tânia Cruz

 i3S - Health Research and Innovation Institute

William Cawthorn

 The Queen's Medical Research Institute, Edinburgh BioQuarter

Alan G Ramsay

 King's College London, Guy's Cancer Centre, Great Maze Pond

Maria J. Oliveira

i3S - Health Research and Innovation Institute

Ricardo Ribeiro

i3S - Health Research and Innovation Institute

Research Article

Abstract

Background

Excessive adiposity, or obesity, has been associated with cancer promotion, including an increased risk for developing Hodgkin Lymphoma (HL). However, the association between obesity and survival in HL can be somewhat paradoxical and may indeed influence prognosis. Examining the bone marrow (BM) cytokine profile in HL patients could provide insights into the mechanisms underlying the altered association between excess adiposity and HL. The BM is an important site for hematopoiesis and can be influenced by various factors, including disease processes and systemic metabolic changes associated with obesity.

Methods

From our cohort, we analyzed interstitial marrow fluid (IMF) from BM aspirates of 16 HL patients at diagnosis and 11 control subjects. Participants were then matched by sex, age, and Body mass index (BMI) for inclusion in our discovery protein array analysis (n = 8 HL and n = 8 donors). We validated our findings in the total sample by measuring adipokine-related molecules using ELISA. Adiposity was measured through abdominal circumference measurement and BMI. Gene expression analysis was conducted through RT-qPCR. Activated signaling pathways were analyzed using HL cell line (L428 cells). Statistical analyses were performed using SPSS and GraphPad.

Results

The IMF of HL patients presented downregulation of interleukins (IL-1α/β, IL-6sR, IL-12), chemokines (CCL2, CCL3, CCL16), IGF-axis mediators (IGFBP-1, IGFBP-2, IGFBP-3, IGF-1sR), sTNFRII, TGFβ1, leptin, osteoprotegerin (OPG), and Fas compared to healthy donors and after controlling for adiposity status. Interestingly, HL overweight/obese subjects showed up-regulation of OPG and lymphotactin in IMF. The results were confirmed by quantification of cytokines, where we observed lower levels of insulin growth factor binding protein IGFBP-3 and higher levels of OPG levels in HL patients. The high-molecular weight (HMW) and total of adiponectin levels were high in HL BM. We further demonstrate that *LEPR*, *TGFβ1*, and *IGFBP3* transcripts were upregulated in fractionated BMAd from HL compared to controls, while *IFG2R* was upregulated in SC. Finally, we observed a possible modulation of L428 cells through IGFBP-3 in an IGF-1-dependent manner, which could be reflected in the BM TME of HL disease.

Conclusions

Our data supports a role for the insulin axis in the BM microenvironment of obese HL patients, particularly through the regulation of insulin ligand-binding proteins.

Background

Obesity has been associated with cancer progression (1). In Hodgkin Lymphoma (HL), a recent large population study revealed a 10% increase in the incidence of Hodgkin's lymphoma (95% confidence interval: 2–19) with each 5 kg/m2 rise in Body Mass Index (BMI) (2). More recently, epidemiological data revealed an association of obesity prevalence with incidence and mortality of HL (3). Albeit obesity increases the risk for developing HL disease, the association with survival seem paradoxical, likely influencing prognosis. In HL patients under chemotherapy, adiposity was associated with better prognostic risk profile, and improved cause-specific survival (4). Excessive adiposity can regulate immune function and impact HL (5). HL has a unique pathological feature characterized by a minority of malignant Hodgkin and Reed-Sternberg cells (HRS) (0.1-1%) and non-neoplastic surrounding cells that express a number of receptors for growth factors and cytokines/chemokines that influence HL growth and progression (6). In lymph nodes (LN), adipokines/cytokines can induce paracrine effects on HRS cells by directly binding to cell receptors or indirect effects driven by altered interactions with tumor microenvironment (TME) LN cells and crosstalk with HRS cells. This network is involved in autocrine/paracrine stimulus in HRS cells, and for maintenance of a microenvironment that fosters immune evasion (7). The HL´s TME components include increased T-helper (Th)2-polarized cells, and regulatory T-cells (Treg), but a paucity of Th1-skewed T cells and cytotoxic T cells (CTL), and natural killer (NK) cells (8).

HL is usually confined to the LN, but bones are common extra-lymphatic sites of HL metastasis (9). In this specific niche, bone marrow adipocytes (BMAds) represent over 10% of total adipose tissue mass. In humans, BMAd is considered to occupy 50 to 70% of the BM volume by early adulthood (10). Concerning the endocrine effects of obesity on cancer cells, the excessive adiposity may modulate HRS aggressiveness in LN through a systemic effect mediated by adipokines and/or migration of adipose stem cells. Metastatic bone involvement in HL, which presents as an osteolytic process, has been described to occur in 5–14% of patients at diagnosis (11). However, the percentage of cases with bone marrow infiltration is likely to be higher as revealed by studies using a more sensitive method of detection (positron emission tomography-computed tomography, PET-CT) compared with bone marrow biopsy (12, 13). Intriguingly, the role of BMAd is currently unknown, although we hypothesize, considering their effector roles in the marrow (described in (5)), that they could modulate the TME. BMAds stimulate osteoclast differentiation and activity by directly secreting the receptor activator of the nuclear factor kappa-B (RANK).

The RANK and its ligand (RANKL) are known to play important roles in regulating bone remodeling and immune responses. Their involvement in HL suggests potential implications for cellular infiltrate, cytokine/chemokine secretion, and overall disease pathogenesis (14). Furthermore, other cytokines are secreted at high levels in the bone marrow, such as leptin and IL-6, in contrast to IL-1β and TNF-α that show low levels of expression (14, 15). In an obesity-associated cancer, the insulin-like growth factor (IGF) system has a pivotal role, including hematological malignancies such as multiple myeloma (16).

Here, we sought to characterize the bone marrow TME according to obesity and pathological status, and to uncover the role of adipokines, and specially the IGF axis, in HL aggressiveness.

Methods

Patients, sample collection and processing

Iliac crest or sternum BM aspirates and peripheral blood samples were obtained from 16 Hodgkin Lymphoma (HL) patients (mean age of 29.4 ± 1.9 years) diagnosed and treated at the Department of Onco-hematology of the Portuguese Institute of Oncology Porto Centre (IPO Porto) and from 11 BM healthy donors / volunteers (mean age of 29.6 ± 2.5 years), recruited from the Laboratory of Cellular Therapy at IPO Porto, and the Immunotherapy Unit and Clinical Pathology Department of Sta Maria Hospital (CHSM), Lisbon. HL patients were included at the time of the first visit to confirm diagnosis in the Department of Onco-hematology of IPO Porto. One patient was excluded due the histopathological diagnosis of histiocytic sarcoma (Supplementary Fig. 1). Donors were selected to match HL participants by age, sex, and body mass index (BMI). BM and peripheral blood samples were gathered in the morning, and for HL patients the collection was performed at the time of diagnosis and before any treatment. Throughout BM aspiration procedure, conducted by experimented clinical hematologists, the first sample (2–4 mL) was collected into a tube with citrate and immediately inverted. The aspirates were centrifuged in Ficoll gradient (Histopaque, Sigma) at 1500 rpm, room temperature for 30min. The upper layer with floating adipocytes (BMAds) was removed, washed and the isolated adipocytes processed to RNA and stored at -80ºC. The interstitial marrow fluid (IMF) was separated, centrifuged, and stored at -80ºC. Stromal cells were collected from a layer after gradient centrifugation, washed, and resuspended in erythrocyte lysis buffer. Isolated stromal cells' pellet was used for RNA processing and then stored at -80ºC. Plasma and serum were separated from peripheral blood samples and stored at -80ºC.

Anthropometric data included height, weight, and abdominal perimeter, following standardized procedures; briefly, a digital scale and a wall-mounted stadiometer were used for weight and height determination, while abdominal circumference was measured at the midpoint between the lower rib margin and the iliac crest. The BMI was calculated using the formula [weight (kg)/height^2 (m)], and thereafter categorized according to WHO classification as underweight (BMI < 18.5 kg/m^2), normal weight (BMI = 18.5 to 25 kg/m^2), overweight (BMI = 25 to 30 kg/m^2) and obese (BMI ≥ 30kg/m^2). Then, participants were stratified into normal BMI (BMI < 25 kg/m^2) and overweight/obese (OW/OB) (BMI ≥ 25kg/m^2) groups. The waist circumference (WC) cutoffs were based on median of 86.0 cm (< = 86 cm: lower abdominal circumference; >86 cm: higher abdominal circumference). Patients were further stratified using the International Prognostic Score (IPS) (18). All individuals consented to participate by signing a written informed consent. The study was approved by ethics' committees of participating institutions (IPO Porto reference: GOM_PI_2013.03 and CHSM reference: 151/14, Refª DIRCLN – 16JUL2014–228). Research was conducted according to principles of the Declaration of Helsinki.

Multiplex array in interstitial medullar fluid

Initially we used a multiplex array (simultaneous determination of 62 adipokines, AAHADIG18 Obesity Adipokine antibody array G series 1, RayBiotech®) for comparing differences of adipokines in the IMF

between HL patients (n = 8) and Donors (n = 8), and obese/overweight versus normal weight subjects. The calculated minimum sample size for having experimental effect is 8 individuals in each group (with a α = 0.05, β = 0.8, rate = 1.0). Briefly, membranes were initially incubated with blocking buffer under gentle shaking for 30 minutes, followed by overnight incubation with IMF at 4ºC. The membranes were then washed and incubated with a biotinylated antibody cocktail for 2 hours at RT. After another washing step, the membranes were labeled with HRP-Streptavidin for 2 hours. Signal intensity was detected by chemiluminescence after adding the substrate and revealed on X-ray film, using several exposure times.

Quantification of adipokines in interstitial medullar fluid and serum

The IMF collected from participants were used to analyze the most differently expressed adipokines through multiplex array. The adipokines were quantified using ELISAs Kits (RayBiotech) in IMF and serum samples (HL *versus* donors), according to manufacturer instructions. Afterwards, the analysis was extended to 16 HL and 11 donors to assess reliability, and to confirm differences found in the protein array. Furthermore, the levels of total and HMW adiponectin were measured using ELISA (Alpco Diagnostics). The nerve growth factor Beta Subunit (NGF-β) and insulin growth factor 1 (IGF-1) levels were quantified using R&D kits, following manufacturer's instructions.

qRT-PCR from BMAd and SVF fractions

The RNA from BMAds and SVF was extracted using TriPure reagent (Roche Applied Science) and purified with the RNeasy Micro Kit. All RNA samples were treated with DNase I (Qiagen). The RNA concentration was determined in a Nanodrop spectrophotometer and stored at -80ºC. Synthesis of cDNA was performed from 50ng total RNA of isolated BMAds and SVF using Nzytech reagents according to manufacturer's instructions. Reverse transcription PCR conditions included an initial step at 70ºC for 10 minutes followed by a second step at 37ºC for 60 minutes. Transcript amount was analyzed by semi-quantitative real-time PCR (qPCR), in duplicates, using 10 µL reaction volume containing 0.5 µL of complementary cDNA, 5 µL of 2x KAPA Probe Fast and 0.2 µL Rox Low (Roche, KK4702), 4 µL $H_2$0dd for each 10 µL final volume of mix used. Then, the mix was divided in two-halfes and added 0.5 µL of primers/probe per reaction. Reactions were loaded into 96-well qPCR plates and run on an Applied Biosystems 7500 Real-Time PCR System. Primers and probes of target genes were bought from Integrated DNA technologies (IDT) (*ADIPOQ* - Hs.PT.58.39512107, *LEP* - Hs00174877_m1, *LEPR* - Hs.PT.58.20484310, *TGF1* - Hs.PT.58.39813975, *IGF1* - Hs.PT.58.21022358, *IGF1R* - Hs.PT.58.3124838, *IGF2* - Hs.PT.58.39913403, *IGF2R* - Hs.PT.58.4204696, *IGFBP1* - Hs.PT.58.3620731, *IGF2BP3* - Hs.PT.58.41034240, *IGFBP3* - Hs.PT.58.4065867). The glyceraldehyde 3-phosphate dehydrogenase (GAPDH Endogenous Control) primers/probe was acquired from ThermoFisher (Hs00266705_g1). Relative quantification was calculated using the REST 2009 software (Qiagen, Hilden, Germany), and relative mRNA expression expressed as fold increase/decrease.

Zymography from interstitial medullar fluid and serum

IMF and serum were analyzed by gelatin zymography. Protein content was determined using the DC Protein assay kit (Bio-Rad). Ten micrograms of protein were mixed with sample buffer (10% sodium dodecyl sulfate, 4% sucrose and 0.03% bromophenol blue in 0.5 M Tris–HCl, pH 6.8) and separated on 10% polyacrylamide gels containing 0.1% gelatin (Sigma-Aldrich) as substrate. After electrophoresis, gels were washed twice with 2% Triton X-100. Gelatin gels were subsequently incubated for 16 hours at 37ºC in 50 mM Tris–HCl, pH 7.5 and 10 mM CaCl2. Gels were stained with 0.1% Coomassie Brilliant Blue R-250 (Sigma-Aldrich), 50% methanol and 10% acetic acid (Merck). MMP-2 and MMP-9 band size and activity were estimated through densitometry analysis (ImageJ2, version 2.3.0).

Proliferation and apoptosis in HL cell line

The Hodgkin Lymphoma human cell line L428was a kind gift from Prof. Nuno Rodrigo dos Santos (Intercellular Communication and Cancer Group, from i3S-Instituto de Investigação e Inovação em Saúde, University of Porto). Testing and authentication of the cell line was conducted using Short Tandem Repeat analysis in DNA with POWERPLEX 16 HSkit (Promega). Cell lines were maintained in RPMI-1640, with 10% of FBS (Gibco BRL). Cells were repeatedly tested for mycoplasma infection during the time flow of experiments.

For the functional studies, $5*10^5$ cells per ml were cultured in duplicate with RPMI 1640 without serum for 24 hours. Then, cells were treated for 72 hours with different concentrations of human proteins (rh) IGF-1 (Abcam ab9573), IGFBP-3 (sigma SRP3067), rh-Adiponectin (Acrp-30, 450 – 24, Peprotech), and rh-Adiponectin globular (gAdiponectin, Cedarlane, CLCYT615-2, 25ug). Apoptosis experiments were conducted after 72 h of stimulation using BD Pharmingen™ FITC Annexin V Apoptosis Detection Kit I (reference: 556547). Cells were collected, washed in binding buffer 1x (BD Biosciences) and incubated with 5 µL of 50 ug/mL of PI (BD Biosciences, 51-66211E) and 2 µL AV (FITC, Immunotools, Cat nº 31490013) for 15 minutes in the dark. In proliferation experiments, L428 cells were labelled with 5nM Carboxyfluorescein N-hydroxysuccinimidyl ester (CFSE) before stimulation with rh-GF-1 and rh-IGFBP-3. We analyzed the proliferation rate after 72 hours of incubation. Over 10.000 cells were examined in the flow cytometer Canto II, and results were analyzed using Flow Jo.

Immunofluorescence of HL cell line

L428 cells were placed on glass coverslips and then fixed with 4% paraformaldehyde (PFA), permeabilized with 0.1% Triton X-100, blocked with 10% FBS, and incubated overnight at 4°C with anti-rabbit primary antibodies anti-ADIPOR1 (1:50, ab126611; Abcam), mouse anti-ADIPOR2 (1:100, sc-514045; Abcam), and sheep IGFBP-3R/TMEM219 (1:1000, AF7556; R&D System). Then, cells were incubated for 1 hour at room temperature with secondary antibodies Goat anti-rabbit Alexa 488 (1:500, A-11008; Invitrogen), Goat anti-mouse Alexa 488 (1:200, A-11029; Invitrogen), and anti-sheep 568 (A21099, Invitrogen). Later, coverslips were washed three times for 5 min in PBS and mounted in microscope slides with Vectashield Mounting Medium with DAPI (Vector Laboratories, Burlingame, CA, USA). Images were acquired with a laser scanning confocal microscope Leica TCS SP5II using a HCX PL APO CS 63x 1.40 OIL UV objective.

Western Blot

Cell lines were starved in medium without serum for 24 hours and treated with different concentrations of rh IGFBP-3 (sigma SRP3067) and IGF-1 (abcam ab9573) for 1 hour. After that, cells were lysed in RIPA buffer (1% NP-40, 150 mM NaCl, 50 mM Tris-HCl pH 7.5, 2 mM EDTA), supplemented with a mixture of protease and phosphatase inhibitors (10 μg/mL NaF, 20 μg/mL Na3VO4, 10 μg/mL PMSF, 10 μg/mL Aprotinin, 10 μg/mL Leupeptin and 50 μg/mL Na4P2O7). Protein content was quantified using the DC protein assay Kit (Bio-Rad) following the manufacturer protocol. Absorbance was determined at 655 nm using SynergyTM Mx fluorometer. For western blot (WB) analysis, 25 μg of protein were mixed in loading buffer 4x (0.25 M Tris-HCl pH 6.8, 9.2% sodium dodecyl sulphate (SDS), 40% Glycerol, 5% (v/v) β-mercaptoethanol and 5% (w/v) bro-mophenol blue) and denatured at 95°C for 5 min. Samples were separated in a 10% SDS-polyacrylamide gel (375 mM Tris-HCl pH 8.8 SDS 0.4%, 0.1% TEMED, 0.05% APS) and transferred to a nitrocellulose membrane (GE Healthcare, Chicago, IL, USA). Membranes were blocked with 5% milk or 4% BSA in phosphate-buffered saline with 0,1% Tween 20 (PBS-T) and incubated overnight with primary antibodies anti-akt (pan 1E7, cell signaling), anti-phospho-akt (ser473, cell signaling), phospho-p44/42 MAPK (Erk1/2) (Thr202/Tyr204, cell signaling), anti-44/42 MAPK (Erk1/2, cell signaling), anti-mTOR (7C10, cell signaling), anti-phospho-mTOR (S2448, cell signaling) and beta-actin (sc47778, Santa cruz).

Statistical analysis

Departure from normality was tested using Shapiro-Wilk test. Then, accordingly, parametric, or non-parametric tests were used to compare differences among variables. Independent samples t-test and Mann Whitney were used whenever variables were non-parametric. Determination of the Spearman or Pearson correlation coefficient was applied to test the strength of association between continuous variables. Specifically for multiplex array, quantile normalization was performed and LIMMA used for differential analysis (19). Signal intensities (intensity by millimeter squared) were calculated using 2-D densitometry software, in agreement with manufacturer's instructions. MCP-3 and TNF-α were excluded from the protein array data due to missing or negative values. Then, array data was log2-transformed to become normally distributed. Statistical analyses on array data were performed using LIMMA R package, and the adjusted P-value was considered statistically significant when < 0.1. Other statistical analyses were conducted using SPSS 21.0 or GraphPad Prism 8. P-values below $p < 0.05$ were considered statistically significant.

Results

Demographics and baseline clinical characteristics

Demographic and clinicopathological data from HL and donors are depicted in Table 1. No differences were observed among disease and control groups. Participants were then matched by sex, age, and BMI for inclusion in our discovery protein array analysis (n = 8 HL and n = 8 donors). Within each group

organized by disease status, we further verified equal distribution by obesity status (n = 4 NW and n = 4 OW/OB), and that normal weight group presented significantly lower BMI compared to the overweight/obese one (Table 1).

Table 1
Participants clinicopathological information's.

	Donors (n = 11)	HL (n = 16)	P-value *
Age, years	29.6 ± 2.5	29.4 ± 1.9	0.951
Gender			
Women	6 (54.5)	10 (62.5)	0.679
Male	5 (45.5)	6 (37.5)	
Height, cm	167.9 ± 3.3	170.4 ± 1.7	0.477
Weight, Kg	72.0 ± 5.9	72.7 ± 3.2	0.906
WC, cm	84.8 ± 4.2	89.0 ± 3.0	0.402
Low	8 (72.7)	6 (37.5)	0.120
High [a]	3 (27.3)	10 (62.5)	
BMI, Kg/m^2	25.3 ± 1.5	25.1 ± 1.1	0.906
NW (18.5−25)	6 (54.4)	11 (68.8)	0.453
OW/OB (≥ 25)	5 (45.5)	5 (31.3)	
Stages [b]			
I + II	-	11 (68.8)	-
III + IV	-	5 (31.3)	-
Histopathology			
Nodular sclerosis	-	13 (81.3)	-
Lymphocyte predominance	-	3 (18.8)	-
B-symptoms [c]			
Yes	-	4 (25.0)	-
No	-	12 (75.0)	-
IPS risk score [d]			
Good	-	10 (62.5)	-
Fair	-	6 (37.5)	-
Poor	-	0 (0.0)	-
Treatment			

	Donors (n = 11)	HL (n = 16)	P-value *
ABVD	-	3 (17.6)	-
ABVD + RT	-	14 (82.4)	-

Disease status and obesity impact adipokine profile in the BM microenvironment.

Analysis of the adipokine protein array (Fig. 1, A) in the discovery set revealed that the IMF of HL patients yielded significantly decreased expression of several interleukins ((IL-1α, IL-1β, IL-8, IL-12), insulin axis proteins (IGFBP-1, IGFBP-3), tumor growth factor β1 (TGF-β1) and leptin, in comparison with donors (Fig. 1, B.**1**). Lower expression in the IMF of HL subjects was maintained for IL-1α and IL-1β, IGFBP-1, IGFBP-3, and for the chemokine stromal cell-derived factor-1 (SDF-1), when only overweight/obese (OW/OB) participants were included in the analysis (Fig. 1, B.**2**). Considering WC or BMI as obesity measure, in the high WC group and OW/OB, IGFBP-3 remained decreased in the marrow of HL patients (Fig. 1, B.**2**). Conversely, comparison of HL with donors, within normal weight (NW) individuals, resulted in unaltered adipokine profile (Supplementary Fig. 1).

Within the HL group, OPG expression was upregulated in OW/OB, whereas insulin, IL-11, XCL1 and the pro-angiogenic vascular endothelial growth factor A (VEGFA) expression was elevated in the high WC group (Fig. 1, C1). Nevertheless, the comparison of obesity status only for donors resulted in unaffected adipokine expression profile (data not shown). Therefore, we moved on to the analysis of extreme groups, HL with OW/OB in relation to NW donors, that supported the putative involvement of IGF axis (downregulation of IGFBP-2 and IGFBP-3), interleukins (IL-8 and IL-1β) and decreased Fas (CD95) protein in the BM of OW/OB HL subjects (Fig. 1, C.**2**). When grouped by obesity status, the OW/OB and the high WC groups had significantly higher levels of the osteoprotegerin (OPG) and the inflammatory chemokine lymphotactin (XCL1), respectively (Fig. 1, D). As adiponectin blots were oversaturated and unreliable to compare among groups within the array, we performed ELISA quantification of total and high molecular weight (HMW) adiponectin isoforms (Fig. 1, E.**1**). The HL patients presented higher IMF levels of total adiponectin and HMW isoform in comparison with donors, even when considering OW/OB status, and extreme groups (HL with OW/OB in relation to NW donors) (Fig. 1, E.**1** - E.**3**), but for the last two, only statistically significative for HMW adiponectin isoform.

Molecular characterization of BM niche and peripheral blood in Hodgkin Lymphoma patients

Altered adipokines from the array were further verified using ELISA in an expanded set of n = 27 subjects (11 donors and 16 HL), to replicate the exploratory findings in IMF and to match with circulating serum levels.

In agreement, IGFBP-3 levels were significantly lower in the IMF of HL patients versus donors (Fig. 2, A.**1**), within NW subjects (HL *versus* donors) (Fig. 2, A.**2**), and among extreme groups, as OW/OB HL patients in

comparation to NW Donors (Fig. 2, A.**4**). For the same comparison (HL *versus* donors), but within OW/OB, we didn´t observed any association (Fig. 2, A.**3**). On the other hand, the OPG was increased in HL patients without obesity (Fig. 2, A.**2**). Beyond these cytokines, the levels of HMW of adiponectin in the BM were higher in HL and HL with OW/OB *versus* donors and donors with different obesity status (NW or OW/OB) (Fig. 2A.**4 - A.6**). But the total adiponectin levels were higher in HL and HL with OW/OB but only when compared with donors without OW/OB (Fig. 2A.**4 - A.6**). Additionally, NGF-β levels were decreased in HL patients (Fig. 2A.**7**), even when HL with obesity (Fig. 2A.**8**), although a tendency was also observed for IGF-1, not statistically significant differences were observed (Fig. 2, A.**9**).

From the peripheral blood, serum IL-8 and IGFBP-1 were significantly lower in HL (Fig. 2, B.**1**), and IL-8 was significantly lower in the serum of HL NW patients than in the serum of NW donors (Fig. 2, B.**2**). The circulating hepatocyte growth factor (HGF) levels were elevated in HL, comparing to donors, even in obesity analysis (Fig. 2, B.**1 to B.3**), with exception for extreme group (Fig. 2, B.**4**). Furthermore, serum matrix metalloprotease-9 (MMP-9) levels were also elevated in HL, comparing to donors (Fig. 2, B.**1 to B.2 and B.4**), in all conditions with exception for obesity group (Fig. 2, B.**3**). Being MMP´s important regulators of several soluble factors, we investigated the activity of MMP-9 and MMP-2 in IMF in our clinical cohort through gelatin zymography (Fig. 2, C.**1**). Interestingly, besides the altered expression, no statistical differences were observed regarding the activity of both metalloproteases among groups by pathology, or obesity status (Fig. 2, C.**2 and C.3).**

As expected, BMI and waist circumference were directly correlated (r = 0.908, P < 0.001) (data not shown), so we analyzed the mentioned cytokines accordingly waist circumference (median of 86 cm). Interestingly, we can confirm some markers, namely, the lower levels of IGFBP-3 and NGF-β, and higher levels of adiponectin (HMW and total) for the HL patients with higher waist circumference versus the donor's counterparty (data not shown). These profiles were also observed for HL patients versus donors without obesity phenotype (data not shown). When considering the high waist circumference, adiponectin levels (HMW and total), continue to be higher among HL patients (data not shown).

In HL patients a positive and significant correlation between bone marrow microenvironment-derived IMF and circulating levels was observed for IGFBP-1, leptin and OPG (Fig. 4, C). Within HLs (n = 16) we analyzed the putative association between IMF and serum levels with clinicopathological characteristics. Adipokine abundance was not related with histopathological subtypes, clinical staging, or presence of B symptoms (data not shown).

The cellular content of bone marrow aspirate was fractionated into adipocytes and stromal vascular fraction (SVF). Bone marrow-derived adipocytes (BMAd) from HL subjects had significantly higher expression of *LEPR*, *TGFB1* and *IGFBP3* mRNA transcripts comparing to donors (Fig. 3, A.**1, A.3**). But with obesity, we observed different profile, namely higher expression of *LEPR* and *IGFBP3* for HL patients with OW/OB in relation to normal weight donors (Fig. 3, A.**2**). When considering all obese, the IGF-1 and IGF-1R mRNA transcripts were increased (Fig. 3, A.**4**). For the stromal vascular fraction (SVF), the IGF-axis was

deregulated, particularly the receptors. The *IGF1R* and *IGF2R* were overexpressed in HL, and *IGF1R* was overexpressed in OW/OB HL subjects (Fig. 3, B).

Altogether, our data suggest that in soluble factors, as IGF1, IGFBP3 and adiponectin, present at IMF or in the serum might be associated with disease and/or adiposity status. Therefore, we tried to deepen the possible relationship and interaction pf these proteins in the HL disease in a metastatic microenvironment, that is, with the cancer cells present.

IGF-axis and adiponectin signaling pathway on HL cell line.

L428 HL cell line expresses IGFBP-3R (TMEM219), IGF-1R and adiponectin receptors (ADIPO-R1 and ADIPO-R2), which was confirmed by gene expression and immunofluorescence analysis (Supplementary figure). Thus, we used L428 cell line for studying the IGF and adiponectin signaling pathways after serum starvation with IGF-1, IGFBP-3, total adiponectin, and globular adiponectin stimulation.

To understand the role of the IGF axis in HL, the HL cell line L428 was challenged with different concentrations of human recombinant (hr) proteins hrIGF-1 and hrIGFBP-3. RhIGF-1 stimulated cell proliferation, whereas no effect was observed in combination with IGFBP-3 (Fig. 4, A). But the combination of IGFBP-3 and IGF-1 decreased the apoptosis of L428 cells (Fig. 4, B). Moreover, the addition of IGFBP-3 induced the activation of mTOR (Fig. 4, C.**2**) and IGF-1 the activation of AMPK (Fig. 4, C.**3**). Interestingly, the combination of IGF-1 and IGFBP-3 decreased the activation of AKT and ERK (**Figure C.4 and C.5**, respectively). Nevertheless, the addition of adiponectin, full-length protein, and its globular isoform, yielded no significant impact on L428 cell phenotype (data not shown).

Discussion

Beyond the association between obesity and cardiovascular risk, current knowledge supports a link between obesity and incidence of cancer and poorer survival outcomes compared to normal (healthy) weight subjects (20). This evidence highlights the possible impact of obesity and particularly the putative effect of hypertrophied adipocytes in the HL TME.

Distinctive environmental factors, particularly the excess BM adiposity, may influence absolute and relative cellular population distribution at the marrow microenvironment (5). This unbalanced microenvironment might support recruitment of malignant cells, promoting BM metastasis formation, and maintenance of a specific immunosuppressive environment that supports tumor growth (5, 21, 22). As seen in HL, the BM is one of the common sites for metastasis (24). However, the knowledge about the profile of adipokines in the BM fluid from subjects with cancer and/or with obesity remains limited. Therefore, considering the obesity context, we assessed the adipokine profile as a gauge of local adipose tissue activity.

By comparing adipokine's expression in cancer and / or adiposity status, our findings revealed that adipokine expression from several axes were downregulated in the IMF of HL subjects, namely cytokines

(IL-1β, IL-1α, IL-6sR, IL-8, IL-12, Fas/CD95, MIP-1b/CCL4), sTNFRII, chemokine ligands (CCL-2 and CCL-3, CCL-16), IGF (IGFBP-1, IGFBP-2, IGFBP-3, IGF-1sR), leptin, growth factors (TGF-β, FGF-6) and bone remodeling molecules (OPG). Lower levels of pro-inflammatory cytokines were found in the IMF of HL patients, supporting the presence of an immunosuppressive microenvironment. IL-6sR, IL-12 and sTNFRII are associated with inflammatory processes at the BM HL niche and have been detected in other hematological malignancies, such as myeloproliferative neoplasms (25). IL-6 has been implicated in oncogenesis and metastasis, throughout osteoclast differentiation and consequent release of growth factors, as observed in multiple myeloma (26). IL-12 has been implicated as stimulator of diseases characterized by inflammation-induced bone destruction. This cytokine stimulates interferon-γ (IFN-γ) synthesis through Signal Transducer And Activator Of Transcription 4 (STAT4) activation promoting Th1 helper cells differentiation with important role on cancer treatment, by controlling tumor growth (27). Indeed, treatment with IL-12 transduced BM cells has been shown to impact metastatic prostate cancer (28). Moreover, murine second generation CAR T cells expressing IL-12 were capable of eradicating established B cell lymphoma with a long-term survival rate of ~25% (29), supporting an anti-tumor effect of this cytokine. Findings suggest that decreased expression of IL-12 at HL BM TME might represent an immune escape mechanism. Another immune escape process involves the expression of Fas (CD95) by cancer cells, which modulates apoptosis through binding at T cells ligand Fas-ligand (FasL), inducing T cell death. Here, we observed decreased Fas expression in HL, independently of obesity status, which may be associates with anti-apoptotic signal driven by CD95$^+$ cytotoxic T cells (30).

It is known that immune escape mechanisms of HRS cells are notable, protecting them by inhibition of cytotoxic T and NK cells activity, as well as promoting anti-inflammatory Treg and Th2 cells recruitment and differentiation (31, 32). Therefore, it is acceptable that at the bone marrow niche we found a counter-regulatory mechanism favoring a protective microenvironment for malignant HRS cell seeding, as an immune escape mechanism.

The IGF axis has also been implicated in obesity-cancer association (33). While IGF-1 is produced at the tumor microenvironment and HRS cells express IGF-1R, the ligand also binds to specific proteins to form binary complexes with binding proteins (34, 35). Here, we found a significantly reduced expression of IGBPs – 1, -2 and – 3 at the medullar fluid of HL subjects compared to donors. De-regulation of IGFBPs has also been demonstrated in the BM of multiple myeloma (36). In particular, the IGFBP-3 protein was consistently reduced in the IMF of HL patients, independently of the obesity status, which might result in an increased free IGF-1 levels and availability of this pro-proliferative ligand. To understand the role of IGFBP-3 in the BM TME of HL subjects, we conducted *in vitro* studies using human recombinant IGFBP-3 and IGF-1 proteins. Previous work on L428 cells demonstrated that IGF-1 [16 ng/mL] and [40 ng/mL] induced cancer cell growth (35). However, for IGFBP-3 there is not much evidence in HL cell lines, which prompted us to test the concentration of IGFBP-3 that we found in IMF from HL patients and reported concentrations from healthy subjects (37). We observed a positive proliferative effect of IGF-1 in HRS cells, but this effect was no longer observed when IGFBP-3 was added, suggesting a competitive inhibition effect. Furthermore, we observed that the combination of IGF-1 [16 ng/mL] and/or IGFBP-3 [15

ng/mL] decreased the impact of this insulin growth factor binding protein in apoptosis. In other cancer types, the IGFBP-3 regulated IGF-1 by blocking IGF-1R with implications on transcription level of type 1 insulin-like growth factor receptor (IGF1R), ERK and AKT (38, 39). Furthermore, at protein level, the interaction between IGFBP-3 and IGF-1 decreased the activation of ERK and AKT, although individually, IGFP-3 induced the activation of mTOR and IGF-1 AMPK. It is described that IGFBP-3 interacts with its receptor (IGFBP-3R/TMEM219) inducing apoptosis (40). However, the observed data may be dependent on availability of each molecule or the pleiotropic nature of IGFBP-3, as proposed elsewhere (40).

Interestingly, although lower levels of IGFBP-3 were observed at BM fluid, its expression may be modulated by BMAds, since we observed a higher mRNA transcript of IGBP-3 in HL patients in relation to donors, excluding in obesity groups (HL OW/OB versus Donors OW/OB). It has been previously described that *IGFBP3* expression is regulated during adipocyte differentiation by interfering with the PPAR gamma-dependent processes (41). Remarkably, an increased expression of IGFBP-3 in the BM has been reported to facilitate bone metastasis by increasing TGF-β-mediated cell proliferation (41). Moreover, the IGFBP-3-modified BM-derived mesenchymal stem cells, promoting apoptosis and downregulating the expression of B-cell lymphoma-2 (Bcl-2), but increasing the expression of the pro-survival Bcl-2 associated X protein in human pulmonary artery smooth muscle cells (42). From our cohort, the increase expression of IGFBP-3 and TGF-β in adipocytes, suggest that they contribute to the formation of an immunosuppressive microenvironment, although we cannot infer an association to bone marrow invasion.

Bone resorption and bone formation are likely to become affected (23). Concerning obesity, and when patients were stratified by BMI classification, we observed osteoprotegerin (OPG) was significantly elevated in the IMF of HL OW/OB compared with lean HLs. OPG is a secreted glycoprotein member of TNF-alpha receptor superfamily, which acts in bone microenvironment as a decoy receptor, binding to RANKL-mediated osteoclast recruitment and activation. Therefore, the increased RANKL/OPG ratio is critical for osteoclastogenesis, by inhibiting osteoclasts differentiation and osteoclastic bone resorption (43). Our findings may reflect a systemic influence of the environment either modulated systemically, by the tumor itself, or through paracrine and/or endocrine mediators from adipocytes and adipose tissue. It is well established that OPG is secreted primarily by osteoblasts but also by adipocytes (44). In conditions of excess adiposity, some reports mentioned increased BMAd count and hypertrophy (45). Adipocytes, normal constituents of the BM microenvironment, were reported to crosstalk with osteoblasts and increase RANKL, while decreasing OPG secretion in the BM, influencing RANKL/OPG ratio through a still unknown mechanism (46). Previous data supports a reduced level of OPG and increased RANKL in the bone marrow of obese mice, which were correlated with higher BM adiposity and upregulated osteoclastogenesis (47, 48). In agreement, previous work revealed higher OPG levels in the IMF of osteoporotic and leaner women (49). Correlating with other cytokines that we found relevant at IMF, the downregulation of pro-inflammatory cytokine IL-11 and VEGF-A may also contribute to inhibition of bone resorption. IL-11R has been suggested as a possible cell surface target for ligand-directed applications in human leukemia and lymphoma (50). On the other hand, VEGF serves as a survival factor for chondrocytes and couples the resorption of cartilage with bone formation during endochondral

ossification. Recently, VEGF has also been found to regulate the balance between osteoblast and adipocyte differentiation in BM mesenchymal stem cells (51).

Beyond the adipo-like molecules described previously, adiponectin is highly enriched at BM microenvironment. Although BM adipose tissue is a source of adiponectin, circulating adiponectin decreases in obese, and insulin-resistant states (52). Since adiponectin exists in distinct multimeric forms including low-molecular-weight (LMW) trimers, middle-molecular-weight (MMW) hexamers, and high-molecular-weight (HMW) complexes, we quantified these isoforms at IMF. We observed higher levels for HL patients with obesity, comparing to donors, which confirms the unfavorable niche for metastasis since low adiponectin levels represents a risk factor for cancer, and for a more aggressive phenotype (53, 54). Furthermore, BMAds of HL patients do express significantly higher levels of adiponectin mRNA. BMAds might be particularly susceptible to such stress, given their relatively high expression of proinflammatory genes and relative resistance to insulin (53). Thus, it seems likely that obesity would also lead to adipocyte dysfunction within the BM, thereby compromising production of adiponectin (55).

Although, we didn´t found a metastatic niche in the studied patients, we found increased serum levels of HGF and MMP-9, precursors of invasion and of metastasis. Evidence reported that the MMP-9 expression by neoplastic cells in HL is associated with EBV positivity (56). This association is correlated with increased serum levels of MMP-9 in HL patients (57). In our study, we also found increased serum levels of MMP-9, a matrix metalloproteinase regulator, involved on degradation of extracellular matrix, growth factors activation and their expression are associated with immune system regulator (58). Notably, treatment with anti-MMP-9 and anti-PDL1 antibodies reduced T-cell receptor clonality and increased TCR diversity (58). Nevertheless, other factors associated with invasion and metastasis, activation of stemness, clonal expansion, and cell transformation, such as HGF and MMP9, were increased in HL patients' serum comparing to controls. This profile seemed to be associated to particularities of the disease, since we found the same profile when considering the normal ponderal subjects, comparing HL patients with controls. Furthermore, the decrease of IL-8, a chemotactic signal for neutrophils, may also indicate a non-reactive infiltrate in HL disease. In line with this, the downregulation of NGF-beta in BM of HL patients seemed to corroborate the decrease differentiation of BM mesenchymal stem cells, thereby diminishing the capability of metastasis (59). The "seed and soil hypothesis" explains the mechanism by which a certain primary cancer metastasis to a specific organ, and according to this theory (60), in Hodgkin Lymphoma disease we might not have good "soil" (bone), for "seed" (cancer cells).

Conclusions

We identified that downregulation of adipokine pathways in the BM are likely modulators of immunoinflammatory (Fas/CD95, IL-12, IL-1 β, IL-8, MIP-1b/CCL4), hormonal (leptin), proliferative (TGF-β, FGF-6 and IGF-axis binding proteins, IGFBP-1, IGFBP-2, IGFBP-3) mechanisms, which ultimately could contribute to the establishment of a metastatic niche in HL. Furthermore, the adipocyte-bone crosstalk, represented by OPG, is likely to impact bone remodeling and consequently the metastatic phenotype.

Finally, our data suggested a role for the insulin axis in the BM microenvironment of obese HL patients, particularly through the regulation of insulin ligand-binding proteins.

Abbreviations

BM	Bone marrow
BMAds	Bone marrow adipocytes
Fas	Fas cell surface death receptor
FGF-6	Fibroblast growth factor 6
FGF-6	Fibroblast growth factor 6
HGF	Hepatocyte growth factor
HL	Hodgkin Lymphoma
HMW	High molecular weight
HRS	Hodgkin and Reed Stenberg Cells
IFN-ɣ	Interferon, gamma
IGF-1 SR	Insulin-like growth factor 1 receptor
IGF-I	insulin-like growth factor 1
IGFBG-1	Insulin-like growth factor-binding protein 1
IGFBP-2	insulin-like growth factor binding protein 2
IGFBP-3	Insulin-like growth factor-binding protein 3
IL-1 alpha	Interleukin 1 alpha
IL-1 beta	Interleukin 1 beta
IL-1 sRI	interleukin Soluble Receptor 1
IL-10	Interleukin 10
IL-11	Interleukin 11
IL-12	Interleukin 12
IL-1α	Interleukin 1 alpha
IL-1β	Interleukin 1 beta
IL-6	Interleukin 6
IL-6 sR	Interleukin 6 soluble receptor
IL-8	Interleukin 8
Insulin	Insulin
Leptin R	Leptin receptor
MCP-1	Monocyte chemotactic protein 2; chemokine (C-C motif) ligand 2

MCP-3	Monocyte chemotactic protein 3
MCSF	Macrophage colony-stimulating factor
MIF	Macrophage migration inhibitory factor
MIP-1beta	Macrophage inflammatory protein beta
MSP alpha	Macrophage stimulating protein alfa
NK	Natural Killer
OPG	Osteoprotegerin
PAI-I	Plasminogen activator inhibitor-1
PARC	parkin-like ubiquitin ligase
RANK	Receptor activator of the nuclear factor kappa-B
RANKL	Receptor activator of the nuclear factor kappa-B ligand
RANTES	Regulated on activation, normal T cell expressed and secreted
Resistin	Resistin
SDF-1	Stromal cell-derived factor 1
STAT4	Signal Transducer And Activator Of Transcription 4
sTNF RI	Tumor necrosis factor receptor I
sTNF RII	Tumor necrosis factor receptor II
SVF	Stromal vascular fraction
TGF-beta	Tumor Growth Factor beta
TNF-alpha	Tumor necrosis factor alfa
VEGF	Vascular endothelial growth factor
XCL1	Monocyte chemotactic protein 1; chemokine (C motif) ligand 1

Declarations

Data Availability

All data generated or analyzed during this study are included in this published article and its supplementary information files.

Author´s Contributions:

AM conceived of the study, execution and drafted the manuscript. JMD, SR, SR, DP, CR, MM, AM, HB, clinical specimen selection and collection. MB helped to draft the manuscript. PZ participated in the data analysis and performed array analysis. FP helped with functional study. WC data analysis and drafted the manuscript. AGR data integration and drafted the manuscript. MJO confirm the authenticity of all data analysis and drafted the manuscript. RR conceived of the study, confirm all data, data analysis and coordination, and helped to draft the manuscript. All authors read and approved the final manuscript.

Acknowledgements:

Corresponding authors:

Dr. Andreia Matos

i3S-Instituto de Investigação e Inovação em Saúde, University of Porto, Porto, Portugal

Rua Alfredo Allen, 208

4200-135 Porto, Portugal

Phone: + 351 96 266 83 94

E-mail: andreia.matos@i3s.up.pt

Professor Ricardo Ribeiro

i3S-Instituto de Investigação e Inovação em Saúde, University of Porto, Porto, Portugal

Rua Alfredo Allen, 208

4200-135 Porto, Portugal

Phone: + 351 91 157 736

Email: ricardo.ribeiro@i3s.up.pt

Ethics declarations

Ethics Committee Approval

This study was based on guidelines of the Declaration of Helsinki and approved by the Institutional Ethical Board of Portuguese Institute of Oncology Porto Centre and Sta Maria Hospital.

Consent for publications

All authors read and approved the final manuscript.

Competing interests

The authors have declared that have no competing interest exists.

References

1. Sung H, Ferlay J, Siegel RL, Laversanne M, Soerjomataram I, Jemal A, et al. Global Cancer Statistics 2020: GLOBOCAN Estimates of Incidence and Mortality Worldwide for 36 Cancers in 185 Countries. CA Cancer J Clin. 2021;71(3):209–49.

2. Strongman H, Brown A, Smeeth L, Bhaskaran K. Body mass index and Hodgkin's lymphoma: UK population-based cohort study of 5.8 million individuals. Br J Cancer. 2019;120(7):768–70.

3. Huang J, Pang WS, Lok V, Zhang L, Lucero-Prisno DE, Xu W, et al. Incidence, mortality, risk factors, and trends for Hodgkin lymphoma: a global data analysis. Journal of Hematology & Oncology. 2022;15(1):57.

4. Landgren O, Andrén H, Nilsson B, Ekbom A, Björkholm M. Risk profile and outcome in Hodgkin's lymphoma: is obesity beneficial? Annals of Oncology. 2005;16(5):838–40.

5. Matos A, Marinho-Dias J, Ramalheira S, Oliveira MJ, Bicho M, Ribeiro R. Mechanisms underlying the association between obesity and Hodgkin lymphoma. Tumour Biol. 2016;37(10):13005–16.

6. Menter T, Tzankov A. Lymphomas and Their Microenvironment: A Multifaceted Relationship. Pathobiology. 2019;86(5–6):225–36.

7. Mulder TA, Wahlin BE, Österborg A, Palma M. Targeting the Immune Microenvironment in Lymphomas of B-Cell Origin: From Biology to Clinical Application. Cancers (Basel). 2019;11(7):915.

8. Ng WL, Ansell SM, Mondello P. Insights into the tumor microenvironment of B cell lymphoma. Journal of Experimental & Clinical Cancer Research. 2022;41(1):362.

9. Mani H, Jaffe ES. Hodgkin lymphoma: an update on its biology with new insights into classification. Clin Lymphoma Myeloma. 2009;9(3):206–16.

10. Suchacki KJ, Cawthorn WP, Rosen CJ. Bone marrow adipose tissue: formation, function and regulation. Current opinion in pharmacology. 2016;28:50–6.

11. Gaudio F, Pedote P, Niccoli Asabella A, Ingravallo G, Sindaco P, Alberotanza V, et al. Bone Involvement in Hodgkin's Lymphoma: Clinical Features and Outcome. Acta Haematol. 2018;140(3):178–82.

12. Kwoun WJ, Ahn JY, Park PW, Seo YH, Kim KH, Seo JY, et al. How useful is bone marrow study as an initial investigative tool without lymph node biopsy in malignant lymphoma?: Eleven years of experience at a single institution. J Clin Lab Anal. 2019;33(4):e22841.

13. Ujjani CS, Hill EM, Wang H, Nassif S, Esposito G, Ozdemirli M, et al. (18) F-FDG PET-CT and trephine biopsy assessment of bone marrow involvement in lymphoma. British journal of haematology. 2016;174(3):410–6.

14. Fiumara P, Snell V, Li Y, Mukhopadhyay A, Younes M, Gillenwater AM, et al. Functional expression of receptor activator of nuclear factor kappaB in Hodgkin disease cell lines. Blood. 2001;98(9):2784–90.

15. Laharrague P, Larrouy D, Fontanilles AM, Truel N, Campfield A, Tenenbaum R, et al. High expression of leptin by human bone marrow adipocytes in primary culture. Faseb j. 1998;12(9):747–52.

16. Bieghs L, Brohus M, Kristensen IB, Abildgaard N, Bøgsted M, Johnsen HE, et al. Abnormal IGF-Binding Protein Profile in the Bone Marrow of Multiple Myeloma Patients. PLOS ONE. 2016;11(4):e0154256.

17. Organization WH. Waist circumference and waist–hip ratio - Report of a WHO expert consultation, Geneva, 8–11 December 2008: World Health Organization; 2011.

18. Moccia AA, Donaldson J, Chhanabhai M, Hoskins PJ, Klasa RJ, Savage KJ, et al. International Prognostic Score in advanced-stage Hodgkin's lymphoma: altered utility in the modern era. J Clin Oncol. 2012;30(27):3383–8.

19. Ritchie ME, Phipson B, Wu D, Hu Y, Law CW, Shi W, et al. limma powers differential expression analyses for RNA-sequencing and microarray studies. Nucleic Acids Res. 2015;43(7):e47.

20. Sahinoz M, Luther JM, Mashayekhi M, Jung DK, Ikizler TA, Engelhardt BG. Hematologic malignancies magnify the effect of body mass index on insulin resistance in cancer survivors. Blood Advances. 2022;6(7):1981–90.

21. Seshadri M, Qu CK. Microenvironmental regulation of hematopoietic stem cells and its implications in leukemogenesis. Curr Opin Hematol. 2016;23(4):339–45.

22. Jalali S, Ansell SM. Role of the Bone Marrow Niche in Supporting the Pathogenesis of Lymphoid Malignancies. Front Cell Dev Biol. 2021;9:692320.

23. Li Z, Bagchi DP, Zhu J, Bowers E, Yu H, Hardij J, et al. Constitutive bone marrow adipocytes suppress local bone formation. JCI Insight. 2022;7(21).

24. Gharbaran R, Park J, Kim C, Goy A, Suh KS. Circulating tumor cells in Hodgkin's lymphoma - a review of the spread of HL tumor cells or their putative precursors by lymphatic and hematogenous means, and their prognostic significance. Crit Rev Oncol Hematol. 2014;89(3):404–17.

25. Chen P, Wu B, Ji L, Zhan Y, Li F, Cheng L, et al. Cytokine Consistency Between Bone Marrow and Peripheral Blood in Patients With Philadelphia-Negative Myeloproliferative Neoplasms. Front Med (Lausanne). 2021;8:598182.

26. Harmer D, Falank C, Reagan MR. Interleukin-6 Interweaves the Bone Marrow Microenvironment, Bone Loss, and Multiple Myeloma. Frontiers in endocrinology. 2018;9:788.

27. Habiba Ue, Rafiq M, Khawar MB, Nazir B, Haider G, Nazir N. The multifaceted role of IL-12 in cancer. Advances in Cancer Biology - Metastasis. 2022;5:100053.

28. Wang H, Yang G, Timme TL, Fujita T, Naruishi K, Frolov A, et al. IL-12 gene-modified bone marrow cell therapy suppresses the development of experimental metastatic prostate cancer. Cancer Gene Therapy. 2007;14(10):819–27.

29. Kueberuwa G, Kalaitsidou M, Cheadle E, Hawkins RE, Gilham DE. CD19 CAR T Cells Expressing IL-12 Eradicate Lymphoma in Fully Lymphoreplete Mice through Induction of Host Immunity. Mol Ther Oncolytics. 2018;8:41–51.

30. Peter ME, Hadji A, Murmann AE, Brockway S, Putzbach W, Pattanayak A, et al. The role of CD95 and CD95 ligand in cancer. Cell Death & Differentiation. 2015;22(4):549–59.

31. Aldinucci D, Gloghini A, Pinto A, De Filippi R, Carbone A. The classical Hodgkin's lymphoma microenvironment and its role in promoting tumour growth and immune escape. J Pathol. 2010;221(3):248–63.

32. Liu Y, Sattarzadeh A, Diepstra A, Visser L, van den Berg A. The microenvironment in classical Hodgkin lymphoma: an actively shaped and essential tumor component. Semin Cancer Biol. 2014;24:15–22.

33. Zhong W, Wang X, Wang Y, Sun G, Zhang J, Li Z. Obesity and endocrine-related cancer: The important role of IGF-1. Frontiers in endocrinology. 2023;14:1093257.

34. Al-Samerria S, Radovick S. The Role of Insulin-like Growth Factor-1 (IGF-1) in the Control of Neuroendocrine Regulation of Growth. Cells. 2021;10(10).

35. Liang Z, Diepstra A, Xu C, van Imhoff G, Plattel W, Van Den Berg A, et al. Insulin-Like Growth Factor 1 Receptor Is a Prognostic Factor in Classical Hodgkin Lymphoma. PLOS ONE. 2014;9(1):e87474.

36. Bieghs L, Brohus M, Kristensen IB, Abildgaard N, Bogsted M, Johnsen HE, et al. Abnormal IGF-Binding Protein Profile in the Bone Marrow of Multiple Myeloma Patients. PLoS One. 2016;11(4):e0154256.

37. Chen HS, Lin HD. Serum IGF-I and IGFBP-3 levels for the assessment of disease activity of acromegaly. J Endocrinol Invest. 1999;22(2):98–103.

38. Ma Y, Han C-c, Li Y, Wang Y, Wei W. Insulin-like growth factor-binding protein-3 inhibits IGF-1-induced proliferation of human hepatocellular carcinoma cells by controlling bFGF and PDGF autocrine/paracrine loops. Biochemical and Biophysical Research Communications. 2016;478(2):964–9.

39. Wang YA, Sun Y, Palmer J, Solomides C, Huang LC, Shyr Y, et al. IGFBP3 Modulates Lung Tumorigenesis and Cell Growth through IGF1 Signaling. Mol Cancer Res. 2017;15(7):896–904.

40. Varma Shrivastav S, Bhardwaj A, Pathak KA, Shrivastav A. Insulin-Like Growth Factor Binding Protein-3 (IGFBP-3): Unraveling the Role in Mediating IGF-Independent Effects Within the Cell. Front Cell Dev Biol. 2020;8:286.

41. Cheng GS, Zhang YS, Zhang TT, He L, Wang XY. Bone marrow-derived mesenchymal stem cells modified with IGFBP-3 inhibit the proliferation of pulmonary artery smooth muscle cells. Int J Mol Med. 2017;39(1):223–30.

42. Chan SS, Schedlich LJ, Twigg SM, Baxter RC. Inhibition of adipocyte differentiation by insulin-like growth factor-binding protein-3. Am J Physiol Endocrinol Metab. 2009;296(4):E654-63.

43. Criscitiello C, Viale G, Gelao L, Esposito A, De Laurentiis M, De Placido S, et al. Crosstalk between bone niche and immune system: osteoimmunology signaling as a potential target for cancer treatment. Cancer Treat Rev. 2015;41(2):61–8.

44. Cao JJ. Effects of obesity on bone metabolism. J Orthop Surg Res. 2011;6:30.

45. Rodríguez A, Ezquerro S, Méndez-Giménez L, Becerril S, Frühbeck G. Revisiting the adipocyte: a model for integration of cytokine signaling in the regulation of energy metabolism. Am J Physiol Endocrinol Metab. 2015;309(8):E691-714.

46. Xu F, Du Y, Hang S, Chen A, Guo F, Xu T. Adipocytes regulate the bone marrow microenvironment in a mouse model of obesity. Mol Med Rep. 2013;8(3):823–8.

47. Gómez-Ambrosi J, Rodríguez A, Catalán V, Frühbeck G. The bone-adipose axis in obesity and weight loss. Obes Surg. 2008;18(9):1134–43.

48. Halade GV, El Jamali A, Williams PJ, Fajardo RJ, Fernandes G. Obesity-mediated inflammatory microenvironment stimulates osteoclastogenesis and bone loss in mice. Exp Gerontol. 2011;46(1):43–52.

49. Pino AM, Ríos S, Astudillo P, Fernández M, Figueroa P, Seitz G, et al. Concentration of adipogenic and proinflammatory cytokines in the bone marrow supernatant fluid of osteoporotic women. J Bone Miner Res. 2010;25(3):492–8.

50. Karjalainen K, Jaalouk DE, Bueso-Ramos C, Bover L, Sun Y, Kuniyasu A, et al. Targeting IL11 Receptor in Leukemia and Lymphoma: A Functional Ligand-Directed Study and Hematopathology Analysis of Patient-Derived Specimens. Clin Cancer Res. 2015;21(13):3041–51.

51. Liu Y, Berendsen AD, Jia S, Lotinun S, Baron R, Ferrara N, et al. Intracellular VEGF regulates the balance between osteoblast and adipocyte differentiation. J Clin Invest. 2012;122(9):3101–13.

52. Cawthorn WP, Scheller EL, Learman BS, Parlee SD, Simon BR, Mori H, et al. Bone marrow adipose tissue is an endocrine organ that contributes to increased circulating adiponectin during caloric restriction. Cell Metab. 2014;20(2):368–75.

53. Scheller EL, Burr AA, MacDougald OA, Cawthorn WP. Inside out: Bone marrow adipose tissue as a source of circulating adiponectin. Adipocyte. 2016;5(3):251–69.

54. Kelesidis I, Kelesidis T, Mantzoros CS. Adiponectin and cancer: a systematic review. Br J Cancer. 2006;94(9):1221–5.

55. Suchacki KJ, Tavares AAS, Mattiucci D, Scheller EL, Papanastasiou G, Gray C, et al. Bone marrow adipose tissue is a unique adipose subtype with distinct roles in glucose homeostasis. Nature Communications. 2020;11(1):3097.

56. Campos AH, Vassallo J, Soares FA. Matrix metalloproteinase-9 expression by Hodgkin-Reed-Sternberg cells is associated with reduced overall survival in young adult patients with classical Hodgkin lymphoma. PLoS One. 2013;8(9):e74793.

57. Hazar B, Polat G, Seyrek E, Bağdatoğlğlu O, Kanik A, Tiftik N. Prognostic value of matrix metalloproteinases (MMP-2 and MMP-9) in Hodgkin's and non-Hodgkin's lymphoma. Int J Clin Pract. 2004;58(2):139–43.

58. Juric V, O'Sullivan C, Stefanutti E, Kovalenko M, Greenstein A, Barry-Hamilton V, et al. MMP-9 inhibition promotes anti-tumor immunity through disruption of biochemical and physical barriers to T-cell trafficking to tumors. PLoS One. 2018;13(11):e0207255.

59. Olechnowicz SWZ, Weivoda MM, Lwin ST, Leung SK, Gooding S, Nador G, et al. Multiple myeloma increases nerve growth factor and other pain-related markers through interactions with the bone microenvironment. Sci Rep. 2019;9(1):14189.

60. Rucci N, Teti A. Osteomimicry: How the Seed Grows in the Soil. Calcif Tissue Int. 2018;102(2):131–40.

Figures
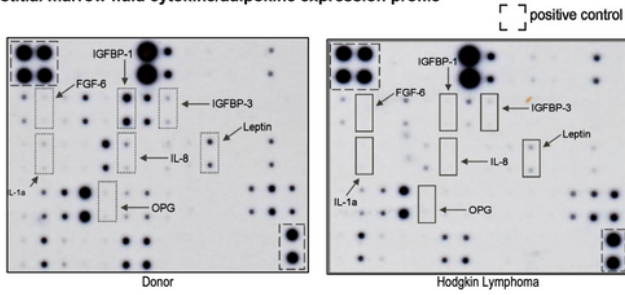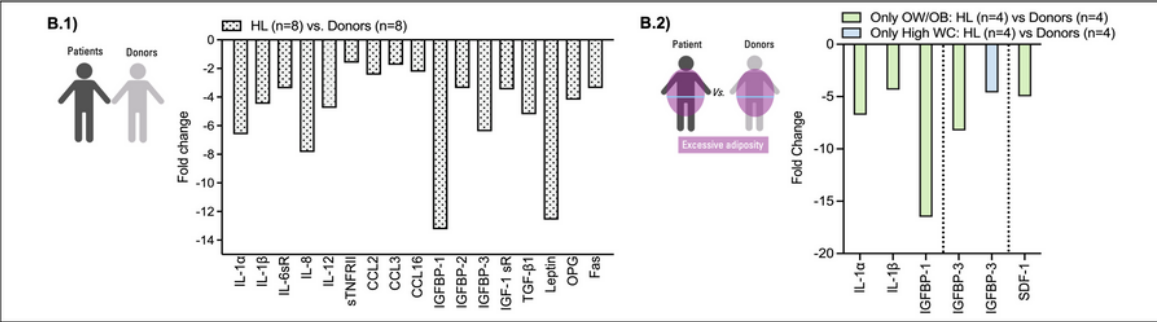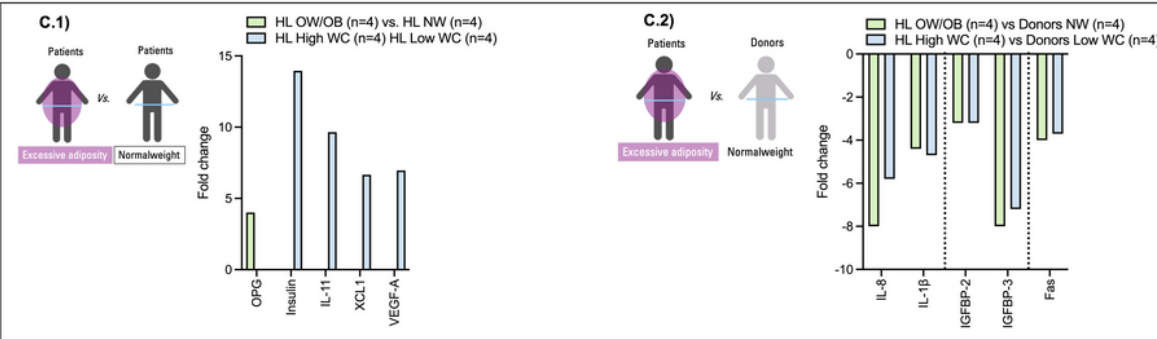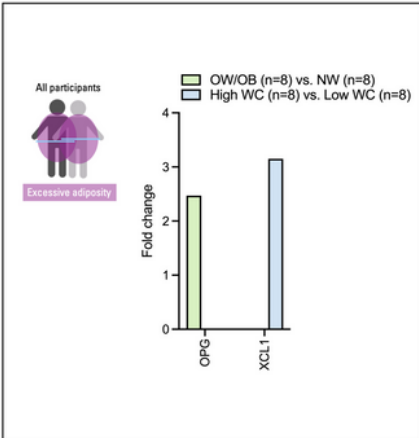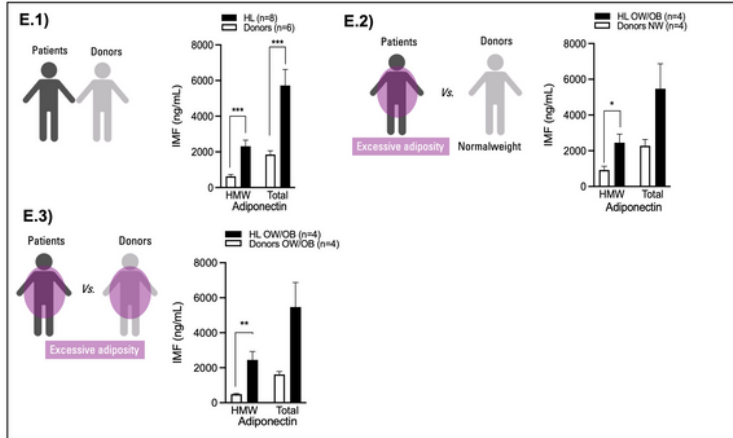
Figure 1

Untangle the interstitial medullary fluid from the adipokine point of view of Hodgkin Lymphoma patients and donors. A) Representative blot membranes of adipokine expression in IMF of one donor and one Hodgkin Lymphoma (HL) patient. **B-D)** Comparison of the amount of adipokines in IMF of donors and HL using an adipokine membrane array. Values represent the fold change and only adipokines with P<0.1 were considered; Differential analysis for the altered adipokines detected from array after quantile

normalization; E) Secretion of total and HMW adiponectin at bone marrow IMF, quantify by ELISA; E.1) HL patients versus donors; E.2) extreme groups: HL OW/OB versus Donor NW. From B to D values represent fold change. For E values represent mean ± SEM and applied the independent t-test. *, P<0.05; ***, P<0.001. IMF, interstitial medullary fluid; HL, Hodgkin's Lymphoma; D, Donors; OW/OB, overweight/obese; NW, normal weight; WC, waist circumference.
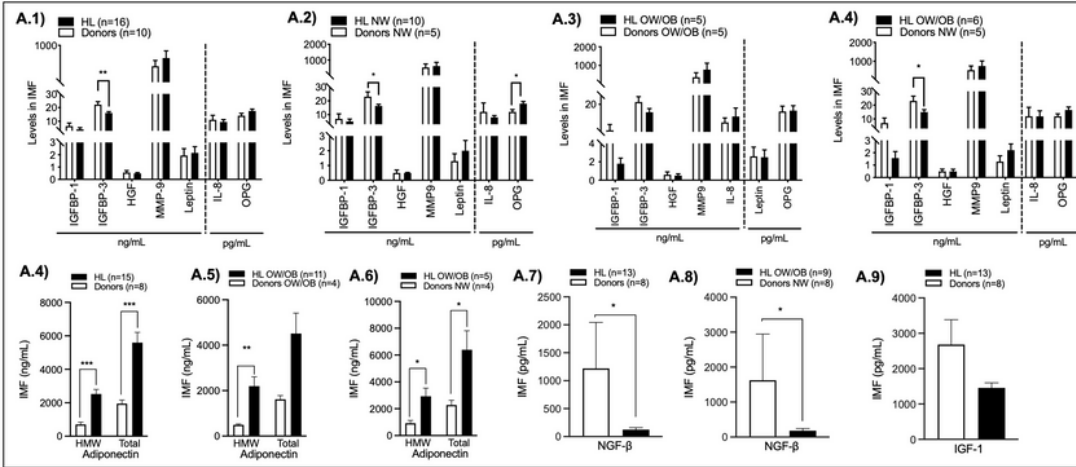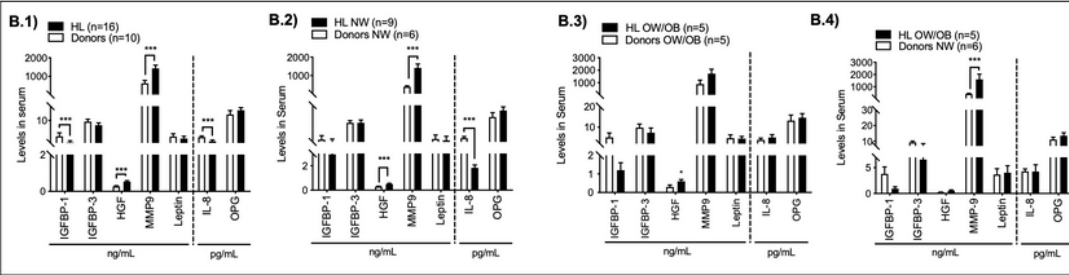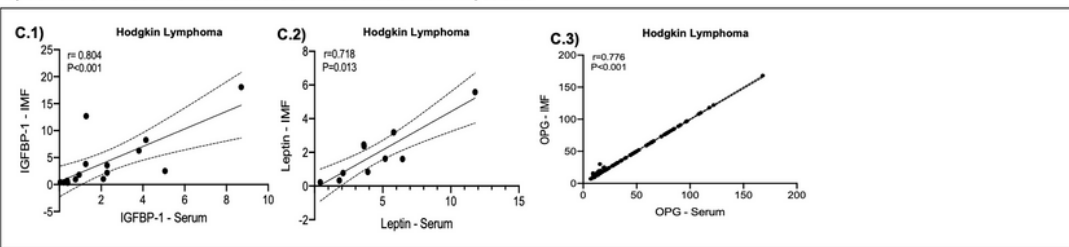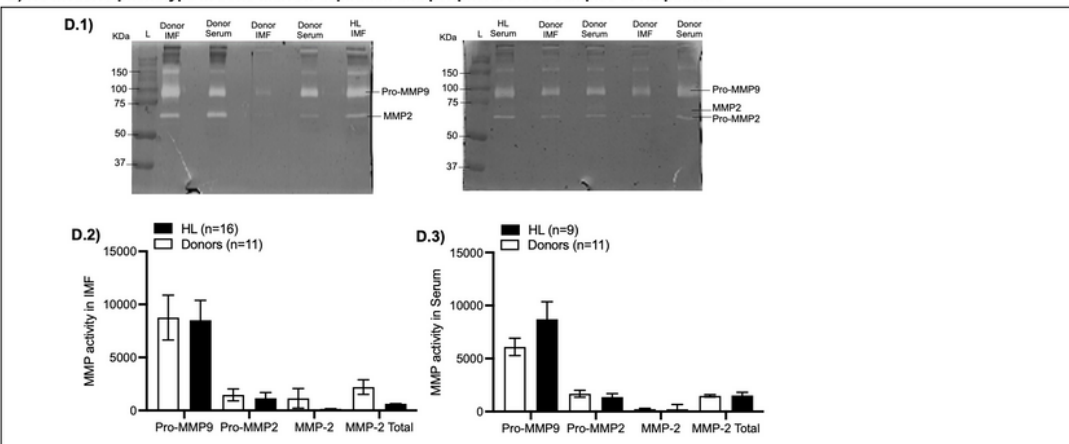
Figure 2

Molecular characterization of Bone marrow niche and peripheral blood in Hodgkin Lymphoma disease.
Quantification in IMF **(A)** and serum **(B)** of the most relevant adipokines from array analysis or from recent literature evidence. **C)** Correlations of IMF and serum levels. **D.1)** shows representative zymograms. **D.2-D.3)** The activity of metalloproteinases (MMP)-9 and MMP-2 were analysed between HL and donors, either from IMF **(D.2)**and serum **(D.3)** samples. Values represent mean ± SEM. Mann-Whitney U test: IGFBP1, IL-8, leptin, HGF, MMP9, adiponectin HMW; Independent t-test: OPG, IGFBP3, total adiponectin. Spearman **(C.1, C.3)** and Pearson **(C.2)** correlations were performed. The dash (—) corresponds to error bars. *, P<0.05; **, P<0.01; ***, P<0.001. IMF, interstitial marrow fluid; HL, Hodgkin's Lymphoma.
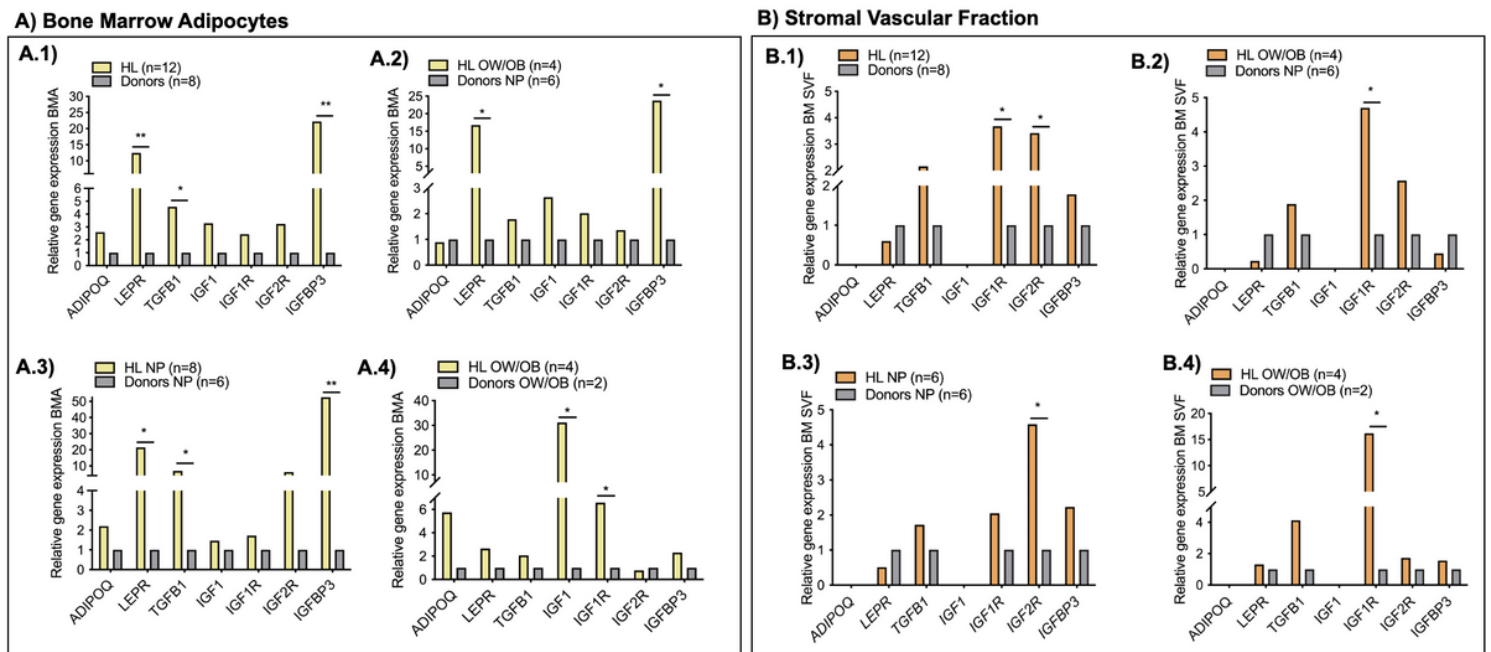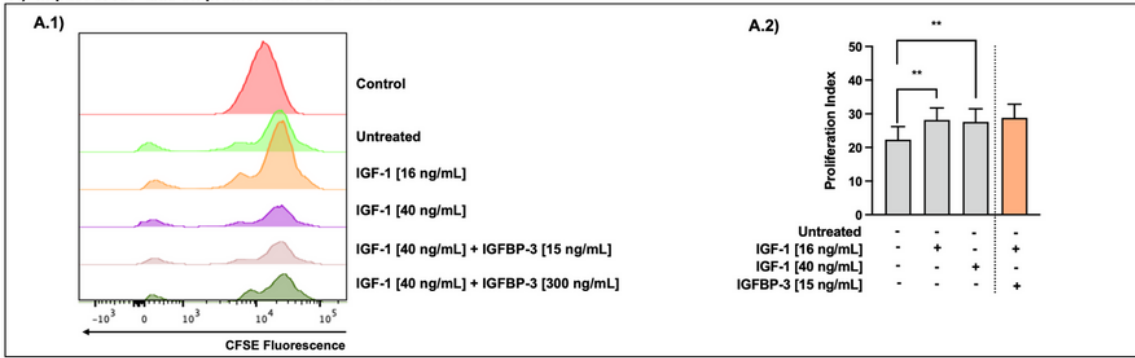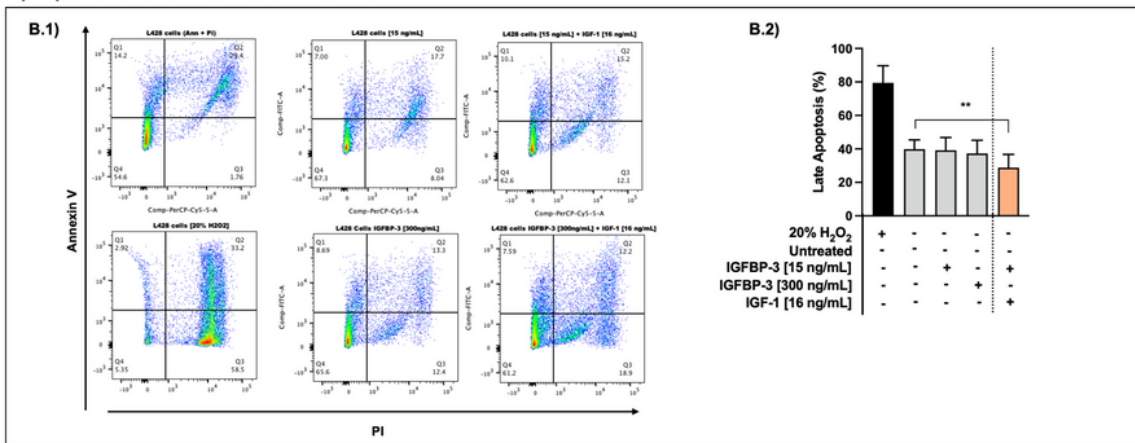
Figure 3

Figure 3

BM adipocytes (A.1, A.2) and SVF (B.1, B.2) are transcriptionally distinct. qPCR analysis of adipocytes and SVF isolated from the bone marrow. Data represent mean. Expression of each target gene was normalized to expression of 18S and GADPH for adipocytes and 18S for SVF. *, P<0.05; **, P<0.01.
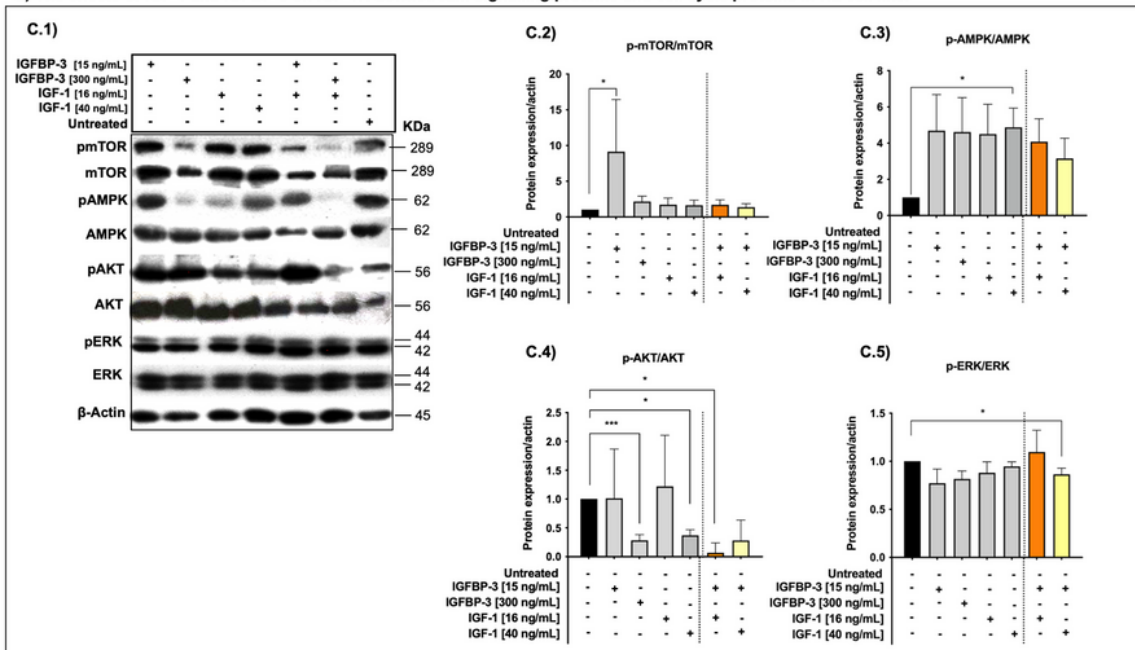
Figure 4

IGF-axis expression and its effect on proliferation and apoptosis of HL cell lines. A) Evaluation of proliferation after incubation 72 hours with different concentrations of recombinant human proteins (rh) IGF-1 and in combination with rh-IGFBP-3, using CFSE. The untreated condition corresponds to L428 cells stained with CFSE and incubated during 72h, without treatment; and the control corresponds to L428 cells incubated with CFSE at the end point of the experiment (A.1) (n=5). **B)** The apoptosis was evaluated

using annexin/pi staining after the incubation of L428 cells with different concentrations of rh-IGFBP-3 and in combination with rh-IGF-1 (n=4). **C)** Phosphorylation and total levels of mTOR, AMPK, Akt and ERK were analysed by western blotting upon IGF-1 and IGFBP-3 stimulation for 1 hour, with different concentrations (n=4). **C.2 to C.5)** Quantification of the proteins analysed by western blotting. *, P<0.05; **, P<0.01; ***, P<0.001. IGFBP-3, insulin growth factor binding protein-3; IGF-1, insulin growth factor.

Supplementary Files

This is a list of supplementary files associated with this preprint. Click to download.

- floatimage1.png